# Raman measurements of substrate temperature in a molecular beam epitaxy growth chamber

T. Hutchins, M. Nazari, M. Eridisoorya, T. M. Myers, and M. Holtz[a)]
*Department of Physics, Texas State University, San Marcos, Texas 78666, USA*

A method is described for directly measuring the temperature of a substrate in a molecular-beam epitaxy (MBE) growth system. The approach relies on the establishment of the temperature dependence of Raman-active phonons of the substrate material using independently known calibration points across the range of interest. An unknown temperature in this range is then determined based on the Raman peak position with the substrate *in situ* the MBE chamber. The apparatus relies on conventional optics and Raman components. Shifting and broadening of the Raman spectrum are described based on the effects of thermal expansion and anharmonic decay. The choice of reference temperature is discussed. The method is qualified by examining the substrate temperature dependence, relative to that of a standard thermocouple, during a commonly used ramp procedure. Both temperature difference and time lag are obtained. © 2015 AIP Publishing LLC. [http://dx.doi.org/10.1063/1.4905858]

## I. INTRODUCTION

Temperature, background pressure, and particle flux are among the key parameters in materials growth and modification. In specific, the temperature used for growth varies across a wide range due to kinetic factors of chemical and physical processes and the particular outcomes desired. This is particularly true for epitaxy, where growth modes, composition, and crystal quality depend on temperature and are process-specific.[1] Accurate measurement and control of temperature are therefore critical during processing.

In molecular-beam epitaxy (MBE), the production of high quality, uniform epitaxial layers generally requires substrate rotation and loading may necessitate a manipulator that vertically translates. Growth uniformity also relies on even heating of substrates. The sample is typically heated by a radiating resistive element recessed within the manipulator housing to illuminate the back surface of the wafer holder or of the substrate itself.[2] A thermocouple (TC) that is either in contact with or located near the sample holder, on the opposite side of the sample, is typically used to assess substrate temperature. This is depicted in Fig. 1(a). While conceptually simple, the implementation of thermocouples in epitaxy chambers is complicated by the availability of positioning options in close thermal association with the growth surface. Due to its recessed location, the thermocouple of a MBE manipulator can at best maintain sample temperature and not provide an absolute reading.

The inherent difficulties in reliably using a thermocouple have motivated non-contact optical methods for *in situ* temperature determination.[3] One common approach is optical pyrometry utilizes blackbody radiation to estimate temperature rise. This requires availability of an optical port to either the substrate holder or back side of the chuck assembly. Limitations arise for pyrometers at low temperatures when deposition-related coating takes place on the surface being interrogated for the measurement or the window, and when the emissivity of the surface (or coating) is either a strong function of pyrometer wavelength or temperature.

More sophisticated optical approaches for measuring temperature inside a MBE system have been developed. Among these are techniques based on the temperature dependence of the semiconductor band edge for the material being deposited[4–6] and either spectroscopic ellipsometry[7] or the related reflectance anisotropy spectroscopy.[8] While each of these methods has its merits, one consideration is the need to know what material is deposited and its temperature-dependent optical properties in the temperature range of interest, limitations in temperature range addressable, and applicability to an arbitrary material.

Raman spectroscopy is a viable approach for determining absolute temperature of a substrate or epitaxial layer for a broad range of materials. The typically narrow Raman bands systematically shift and broaden with increasing temperature and the dependence has been established for many materials. A perceived difficulty in using Raman scattering to examine materials *in situ* is the typically weak signals and the consequent need to use collection optics with high numerical aperture. Despite these factors, progress has been made in measuring Raman spectra with large working distance optics.[9,10] However, application to monitoring semiconductor process parameters has not yet been fully exploited with the majority of attention devoted to the epitaxial material.[11,12] In this work, we demonstrate that conventional optics and commonly available Raman instrumentation permit measurement of temperature in a working MBE system and across a wide temperature range.

## II. RAMAN APPARATUS

Figure 1(b) depicts the custom optical setup used for carrying out the large working distance Raman measurements.
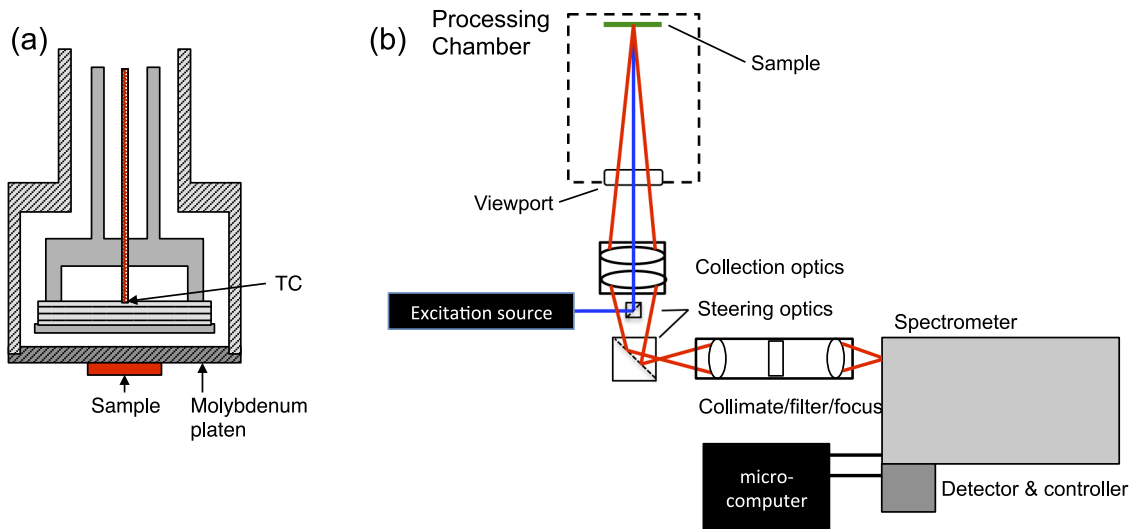
---

a)Mark.Holtz@txstate.edu

FIG. 1. (a) Depicts position of sample on molybdenum platen and the position of the TC. (b) Schematic layout of the Raman apparatus used to measure substrate temperature inside the MBE chamber.

The setup was qualified in a standard laboratory configuration and by substrate measurement in a MBE growth system.[13] The excitation was a solid-state laser operating at 532 nm. Laser-focus and collection optics used a commercial camera objective capable of short working distances (35 cm). This objective focused the laser onto the sample with nominal spot diameter ~1 mm. The distance between the objective and sample in the MBE chamber was 45 cm for this demonstration. Scattered light collected by the camera objective was collimated, passed through a standard notch filter, and focused on the entrance slit of a 0.5-m spectrometer equipped with a 1800 g/mm diffraction grating with maximum throughput (blaze) at 500 nm. Spectrally dispersed light was detected using a liquid nitrogen cooled charge-coupled device (CCD) detector. Wavelength calibration was carried out using a standard neon pen lamp.

## III. CALIBRATION APPROACH AND INTERPRETATION

Calibration of the shift in the Raman spectrum induced by temperature change was conducted using data from the standard laboratory configuration and the MBE setup. A small piece ~1 cm$^2$ of a commercial 6H-SiC wafer (0.3 mm in thickness) was used for this demonstration. The 6H-SiC was (0001) oriented and semi-insulating with nominal resistivity >$10^5$ $\Omega$ cm. Silicon carbide was chosen due to its robustness in the temperature range of interest and the availability of distinct Raman-active phonons. For the laboratory setup, the sample was affixed to a conventional hot plate and temperature determined using a co-located thermocouple approximately 3 mm from the sample. Temperature was varied and spectra collected for off-line data fitting to determine peak position and line width. In the MBE chamber, the sample is mounted to the solid molybdenum chuck using indium. This is in contrast to ring mounts such as what is typically used with whole wafers, such as GaAs or Si, where direct absorption of infrared radiation produced by the heater into the substrate is the principal heating mechanism. Since the wafer holder is solid

in our experiments, thermal conduction through the chuck, indium, and into the substrate primarily heats the sample rather than absorption. The chuck is transferred into the chamber through a load-lock and held mechanically and thermally via a bayonet-style mount. The thermocouple is positioned on the opposite side of the molybdenum platen from the sample, and not in physical (thermal) contact, as depicted in Fig. 1(a).

For calibration of the Raman positions, we used two independently known temperatures with the sample in place. The first is the indium metal melting point at 156.7 °C, the second was the melting temperature of InSb at 527 °C. Both of these melting points were readily confirmed visually and Raman spectra subsequently acquired at these known temperatures for the calibration.

Figure 2 shows Raman spectra of the 6H-SiC at a representative low temperature and the two melting points described above. Integration times for spectra ranged from 1 s to 2 min. Clearly seen are several bands in the 750–810 cm$^{-1}$
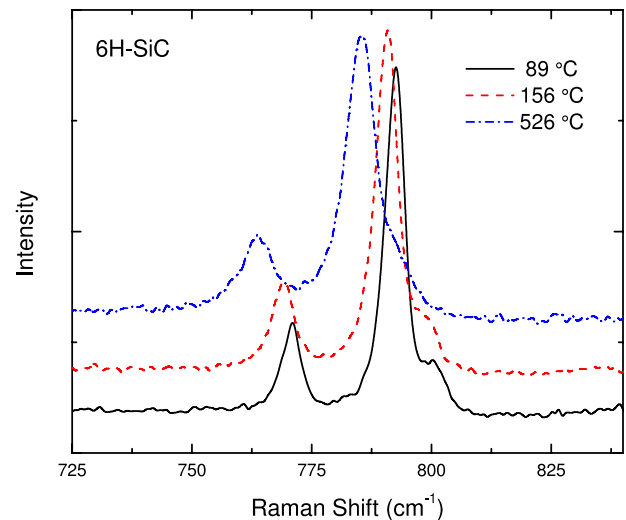


FIG. 2. Raman spectra obtained in the laboratory at several temperatures in the laboratory setup (89 °C) and in the MBE chamber (156 and 526 °C).
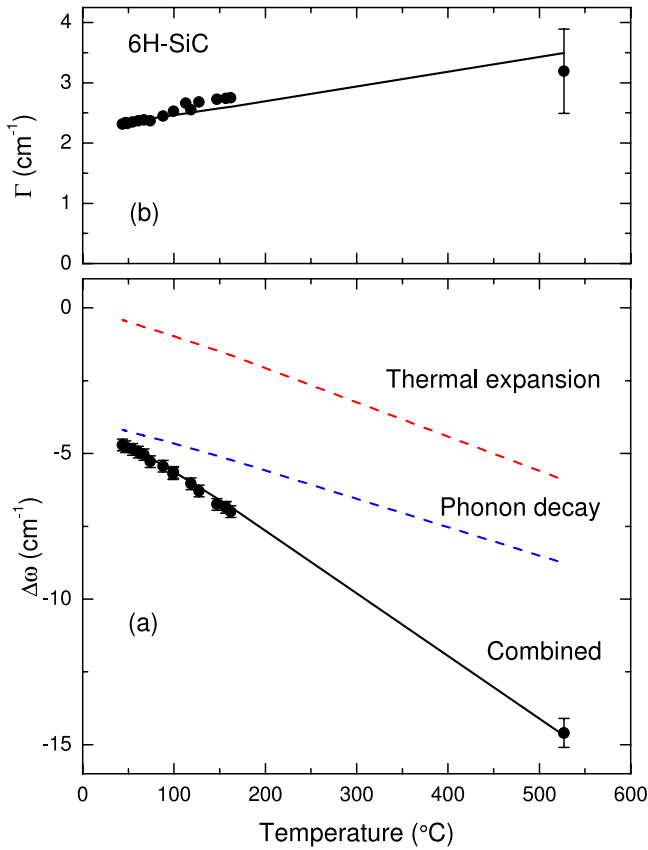
FIG. 3. (a) Temperature dependence of the $E_2$ phonon peak position of 6H-SiC combining data from the laboratory setup and in the MBE chamber. The latter are points at 157 and 527 °C. (b) Temperature dependence of the $E_2$ phonon line width.

range including the sharp $E_2$ line[14] near 793 cm$^{-1}$ (room temperature). As expected, the spectral features systematically red shift and broaden with increasing temperature. Figure 3(a) summarizes the temperature dependence of the shift in peak position, $\Delta\omega(T) = \omega(T) - \omega(T_0)$, for the $E_2$ band and Fig. 3(b) shows the line width ($\Gamma$). Quantity $\omega$ is phonon energy (in cm$^{-1}$) and reference temperature $T_0$ may be arbitrarily chosen; in Fig. 3(a), it corresponds to absolute zero. The observed shift in Raman position may now be applied to estimate an unknown substrate temperature up to 527 °C, based on straightforward interpolation, and judiciously above this range by extrapolation of the dependence. However, extension of the range should involve calibration based on other independently known temperatures in the processing apparatus.

## IV. PHYSICAL BASIS OF THE TEMPERATURE DEPENDENCE

The effect of temperature on phonon energy has been previously investigated for numerous materials including 6H-SiC.[14,15] Shifts are attributed to thermal expansion and the effect of phonon decay. For the zone-center $E_2$ vibration, a symmetric two-phonon decay has been applied to adequately describe the dependence from 20 to 350 K.[15] In this process, the initial phonon of energy $\omega_0$ decays into two phonons each

having energy $\omega_0/2$ and opposite momentum wavevectors

$$\omega(T) = \omega_0 - \omega_0\gamma \int_{T'=0}^{T} [\alpha_c(T') + 2\alpha_a(T')]dT' \\ - A\left[1 + 2n\left(\frac{\omega_0}{2}, T\right)\right], \quad (1)$$

where $\omega(T)$ is the energy (in cm$^{-1}$) at absolute temperature $T$, $\omega_0$ corresponds to the $T = 0$ phonon energy, $\gamma = 1.23$ is the Grüneisen constant for 6H-SiC,[16] and $\alpha_{c(a)}$ is the temperature dependent thermal expansion coefficient along the $c$ ($a$) crystallographic axis of this material taken from the literature.[17] The phonon decay term includes the Bose function defined

$$n(\omega, T) = \frac{1}{\exp\left(\frac{hc\omega}{k_B T}\right) - 1}, \quad (2)$$

where $h$ and $k_B$ are the Planck and Boltzmann constants, respectively, and $c$ is the speed of light. The factor $A$ is a measure of the relative importance of phonon decay to the thermal expansion and is commonly treated as a fit parameter. In Fig. 3(a), we show the result of fitting Eq. (1) to our data. All quantities are taken from the literature except for $\omega_0$, which is related to the phonon energy at absolute zero, and parameter $A$. We obtain $\omega_0 = 792.0$ cm$^{-1}$ and $A = 3.0$ cm$^{-1}$. The value of $A$ obtained here is the same as what has been previously reported for this phonon in 6H-SiC.[15]

When evaluating temperature-induced phonon shift from a particular reference $T_0$, as we do here, several simplifications may be made. The revised shift in phonon energy is

$$\omega(T) - \omega(T_0) = -\omega_0\gamma \int_{T'=T_0}^{T} [\alpha_c(T') + 2\alpha_a(T')]dT' \\ - 2A\left[n\left(\frac{\omega_0}{2}, T\right) - n\left(\frac{\omega_0}{2}, T_0\right)\right]. \quad (3)$$

Above the cryogenic range ($\sim$100 K), where the thermal expansion coefficients vary strongly with temperature, the quantity in square brackets in the second term of the right hand side of Eq. (3) may be factored out of the integral

$$\int_{T'=T_0}^{T} [\alpha_c(T') + 2\alpha_a(T')]dT' = [\alpha_c + 2\alpha_a](T - T_0), \quad (4)$$

where the thermal expansion coefficients now correspond to the high-temperature average across the range between $T$ and $T_0$. Furthermore, in the high-temperature range $k_B T > \frac{hc\omega_0}{2}$, the Bose functions may be approximated by $n\left(\frac{\omega_0}{2}, T\right) \to \frac{2k_B T}{hc\omega_0}$. Combining these factors, Eq. (3) may be simplified to produce a shift linear in temperature

$$\omega(T) - \omega(T_0) = -\left[\omega_0\gamma(\alpha_c + 2\alpha_a) - 4A\frac{k_B}{hc\omega_0}\right](T - T_0). \quad (5)$$

A linear fit to the data in Fig. 3(a) results in a slope of $-0.0208 \pm 0.0005$ cm$^{-1}$/K in good agreement with previously published results for 6H-SiC.[14,15] We note that inclusion of the next term in the approximation of the Bose function results in a correction factor to the linear dependence in Eq. (5)

$$\frac{Ahc\omega_0}{(4k_B)\left(\frac{1}{T} - \frac{1}{T_0}\right)}, \quad (6)$$

which is negative for $T > T_0$. Note that this compact expression is only valid for symmetric decay. Using our value of parameter $A$, the quantity in Eq. (6) is in the order of $-2$ cm$^{-1}$ across the full temperature range of Fig. 3 and the high-temperature limit of this expression is $-3$ cm$^{-1}$ for our data parameters. These are significant fractions of the full $-10$ cm$^{-1}$ shift observed in Fig. 3(a) due to the low $T_0$ used in this analysis. This is not surprising, since the high-temperature limit from the Bose function approximation corresponds to $T \gtrsim 300\,°C$. We may conclude that the use of the linear fit is not adequate for accurately estimating an unknown temperature, based on the Raman peak and using room temperature as the reference $T_0$. The full description in either Eq. (1) or (3) is necessary, although availability of the dependence across the low-temperature range[14,15] is helpful in determining the necessary constants. Better implementation of the linear model is expected when the $k_B T_0 > \frac{hc\omega_0}{2}$ condition is met for the reference temperature. Despite its shortcoming, the simple linear dependence obtained above may be used to estimate an unknown temperature in the range studied here within $\sim 2.5\%$ accuracy.

The temperature dependence of the $E_2$ line width is summarized in Fig. 3(b). As expected and seen in the raw data of Fig. 2, a gradual increase is observed in $\Gamma(T)$. This increase is due to the diminishing lifetime of the zone-center $E_2$ phonon resulting from impurity- and defect-related scattering and the anharmonic decay via phonon-phonon scattering. The temperature dependence may be summarized accordingly in an expression analogous to the last term in Eq. (1)

$$\Gamma(T) = \Gamma_0 + B\left[1 + 2n\left(\frac{\omega_0}{2}, T\right)\right], \tag{7}$$

where parameter $B$ is associated with the relative importance of phonon-phonon interactions and is treated as a fit parameter. Additionally, $\Gamma_0$ is related to the intrinsic scattering rate due, for example, to impurities and native defects in the material. The value of $\Gamma_0$ may therefore be used as an indicator of material quality.[18,19] From our data and Eq. (7), we obtain $\Gamma_0 = 0.4$ cm$^{-1}$ and $B = 1.4$ cm$^{-1}$, both in reasonable agreement with what has been previously reported.[15] We note that the gradual change in the line width of this phonon makes it less suitable than peak position for accurately estimating an unknown sample temperature.

## V. APPLICATION TO STANDARD TEMPERATURE RAMP

Based on this calibration approach and the dependence of the phonon energy in Eq. (3), we may now determine an unknown substrate temperature. To illustrate the importance of absolute Raman temperature measurement to the standard thermocouple, we carried out a simple temperature ramp in the MBE chamber with the 6H-SiC affixed to the wafer chuck. The intended ramp takes the substrate from 150 to 550 °C with a ramp rate of 30 °C/min. Figure 4 compares temperature of the thermocouple, used for control, and the Raman results during the ramp process. Straightforward conclusions may be drawn from comparing these results. First, temperature is overestimated by the thermocouple reading by $\sim 100$ °C.
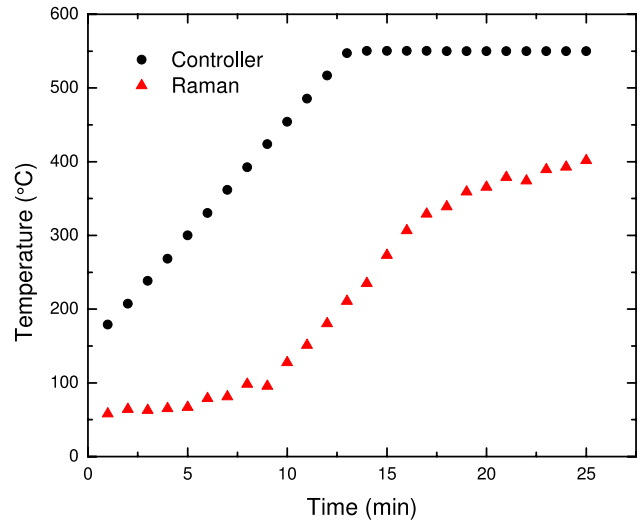


FIG. 4. Comparison of MBE system thermocouple temperature and that obtained from the Raman measurements for a standard ramp-up prior to growth in the MBE chamber. Error bars in the Raman-based temperatures are comparable to the size of the data symbols.

Second, the ramp rate at the substrate (albeit delayed) is comparable to that at the thermocouple, suggesting that parasitic heat losses are a consistent factor for these ramp conditions. Third, there is a time lag as large as 10 min between the thermocouple temperature reaching the set point (550 °C) and the substrate achieving near steady-state conditions at its much lower temperature. An additional 10 min soak resulted in a flat temperature profile at 400 °C but did not address the temperature differences between these two sensing approaches.

## VI. CONCLUSIONS

We have successfully demonstrated an *in situ* temperature measurement based on Raman scattering and implemented it in a standard MBE growth system. The approach relies on conventional apparatus. Calibration was carried out using combined data measured with a representative 6H-SiC substrate in a laboratory setting and MBE system. The available capabilities allowed us to qualify the approach from room temperature to 527 °C. To examine the efficacy of this method for absolute measurement of temperature, we applied it to a standard MBE ramp process. Results show that the thermocouple significantly overestimates the substrate temperature by $\sim 100$ °C and that there is a >10 min delay in achieving steady state at the sample relative to the controller.

Other substrates and epilayers may be used to measure temperature rise in a similar fashion, provided they have distinct Raman bands. This is the case for other semiconductor substrates, although higher Raman shift is generally easier to measure and the precision of the method relies on a high $\frac{d\omega}{dT}$ value. It is furthermore necessary for the material to exhibit distinct Raman features measurable in the temperature range of interest. For these other prospective substrates or epitaxial layers, knowledge of the Raman spectrum and

its temperature dependence are necessary prerequisites for which there is a large database of published work. For situations in which the growing material absorbs the Raman excitation and scatter, the substrate intensity will diminish as the process proceeds. This represents a limiting factor when substrate temperature must be modified after growth conditions are established and the epilayer itself is not viable for temperature measurements.

[1]M. J. Ekenstedt and T. G. Andersson, J. Vac. Sci. Technol. B **9**(3), 1605 (1991).

[2]W. S. Knodle and R. Chow, *Handbook of Thin Film Deposition Processes and Techniques: Principles, Methods, Equipment and Applications*, edited by K. Seshan (Noyes Publications, 2001), p. 381.

[3]F. G. Boebel, H. Moller, B. Hertel, H. Grothe, G. Schraud, S. Schroder, and P. Chow, J. Cryst. Growth **150**(1-4), 54 (1995).

[4]S. Johnson, C.-H. Kuo, M. Boonzaayer, W. Braun, U. Koelle, Y.-H. Zhang, and J. Roth, J. Vac. Sci. Technol. B **16**(3), 1502 (1998).

[5]R. N. Sacks, D. Barlett, C. A. Taylor, and J. Williams, J. Vac. Sci. Technol. B **23**(3), 1247 (2005).

[6]K. Lee and T. H. Myers, J. Electron. Mater. **36**(4), 431 (2007).

[7]M. F. Vilela, G. K. Pribil, K. R. Olsson, and D. D. Lofgreen, J. Electron. Mater. **41**(10), 2937 (2012).

[8]P. Weightman, D. S. Martin, R. J. Cole, and T. Farrell, Rep. Prog. Phys. **68**(6), 1251 (2005).

[9]S. K. Sharma, P. G. Lucey, M. Ghosh, H. W. Hubble, and K. A. Horton, Spectrochim. Acta, Part A **59**(10), 2391 (2003).

[10]L. C. Pacheco-Londono, W. Ortiz-Rivera, O. M. Primera-Pedrozo, and S. P. Hernandez-Rivera, Anal. Bioanal. Chem. **395**(2), 323 (2009).

[11]D. R. T. Zahn, A. Schneider, and D. Drews, J. Raman Spectrosc. **28**(10), 825 (1997).

[12]M. Kuball, Surf. Interface Anal. **31**(10), 987 (2001).

[13]J. Chai, K. K. Lee, K. Doyle, J. H. Dinan, and T. H. Myers, J. Electron. Mater. **41**(10), 2738 (2012).

[14]M. Bauer, A. M. Gigler, A. J. Huber, R. Hillenbrand, and R. W. Stark, J. Raman Spectrosc. **40**(12), 1867 (2009).

[15]I. Ahmad, V. Kasisomayajula, D. Y. Song, L. Tian, J. M. Berg, and M. Holtz, J. Appl. Phys. **100**, 113718 (2006).

[16]J. Liu and Y. K. Vohra, Phys. Rev. Lett. **72**(26), 4105 (1994).

[17]Z. Li and R. C. Bradt, J. Am. Ceram. Soc. **70**(7), 445 (1987).

[18]D. Y. Song, M. Basavaraj, S. Nikishin, M. Holtz, V. Soukhoveev, A. Usikov, and V. Dmitriev, J. Appl. Phys. **100**, 113504 (2006).

[19]D. Y. Song, M. E. Holtz, A. Chandolu, A. Bernussi, S. A. Nikishin, M. W. Holtz, and I. Gherasoiu, Appl. Phys. Lett. **92**(12), 121913 (2008).